Patient-Driven Control of FES-Supported Standing Up: A Simulation Study

Robert Riener, *Associate Member, IEEE,* and Thomas Fuhr, *Student Member, IEEE*

***Abstract*—To control movements aided by functional electrical stimulation (FES) in paraplegic patients, stimulation of the paralyzed lower limbs might be adjusted in response to voluntary upper body effort. Recently, Donaldson and Yu proposed a theoretical approach, called "control by handle reactions of leg muscle stimulation" (CHRELMS), in which stimulation of the lower limbs depends on upper body effort, i.e., body posture and recorded hand reactions, and is aimed to minimize arm forces during standing up and standing. An alternative strategy is presented in this paper, which accounts for voluntary upper body effort as well, but does not require estimation of hand reactions. The objective of this study is to test both strategies by applying them to a generic two-dimensional (2-D) neuromusculoskeletal model. The model takes into account the major properties of muscle and segmental dynamics during FES-supported standing-up movements of a paraplegic patient. In comparison to standing up without FES-support, both closed-loop strategies yield satisfying standing-up movements although no reference information (e.g., a desired trajectory) is required. Arm forces can be significantly reduced. Using the model to optimize the controller, time-consuming and strenuous trial-and-error experimentation could be avoided. However, final experimental studies are planned to verify the presented strategies.**

***Index Terms*— Biomechanical model, control strategies, FES, patient-driven control, standing up, stimulation.**

I. Introduction

FUNCTIONAL electrical stimulation (FES) has been employed by many investigators to artificially activate skeletal muscles and thus partially restore motor function in patients with upper motor neuron lesions [1]–[4]. However, the control of multiple joints by FES is very complex, and effects such as muscle fatigue, spasticity, and limited force in the stimulated muscle further complicate the control task. Therefore, FES applications to standing, standing up, or walking require paraplegic patients to use their arms during the movement to both compensate for limited leg joint moments and to maintain balance.

Voluntary contributions of the trunk and arms are difficult to predict, and thus incorporate in a control strategy. However, if the FES controller does not account for voluntary contributions, artificial and natural control could adversely interfere, resulting in undesired or even dangerous motion and increased upper body effort. To coordinate artificial and voluntary control in a neuroprosthesis, one possible approach is to adjust the stimulation to the estimated voluntary contribution of the patient (e.g., by recording the hand reaction forces). In such a "patient-driven" approach the patient is able to influence or even control the stimulation of the paralyzed limbs of his body. Thus, the patient's CNS is an important part of the controller, as opposed to many other "controller-centered" approaches presented in the literature (e.g., trajectory-tracking, path-following, phase plane control) where the patient has to submit to the controller.

Recently, Donaldson and Yu [5] proposed a strategy which accounts for voluntary upper body effort in the control of FES-supported standing up and standing. In their theoretical approach, stimulation of the lower extremities depends on posture and hand reactions. The goal is to minimize arm efforts. Their strategy is called "control by handle reactions of leg muscle stimulation" (CHRELMS).

In this paper, we propose a different strategy which also accounts for voluntary upper body effort, but does not require estimation of hand reactions. To reduce upper body effort, we compute the stimulation pattern required to maintain the movement initiated by upper body effort. We call this strategy "patient-driven motion reinforcement" (PDMR).

The use of models can significantly enhance the design and test of closed-loop control strategies applied to FES. Thus, trial-and-error adjustments during experiments that are very tiring for the patient can be avoided, or at least shortened, and the number of experiments in humans reduced. The main objective of this paper is to validate both strategies by applying them to a generic two-dimensional (2-D) neuromusculoskeletal model of a subject standing up with the support of FES. The strategies are examined in the light of the following questions: Can closed-loop FES as proposed in the two strategies realize standing up and standing? Can the resulting movement be improved compared to standing up without FES support (arm support only), or open-loop FES support? And, can arm forces be significantly reduced? Additionally, more specific questions are to be clarified: How do arm disturbances or muscle trembling due to high arm forces affect the resulting movement in the different strategies? And, can standing be achieved with the hip, knee, and ankle joints approximately aligned?

Manuscript received September 10, 1997; revised November 17, 1997, December 16, 1997, and January 14, 1998. This work was supported by the Deutsche Forschungsgemeinschaft (DFG), SFB 462 "Sensomotorik," project A1.

The authors are with the Institute of Automatic Control Engineering (Lehrstuhl für Steuerungs und Regelungstechnik), Technical University of Munich, 80333 Munich, Germany.

Publisher Item Identifier S 1063-6528(98)03599-X.

II. Description of the Model

A. Model of a Paraplegic Patient

The model describes major properties of muscle and segmental dynamics occurring during FES. The human body is

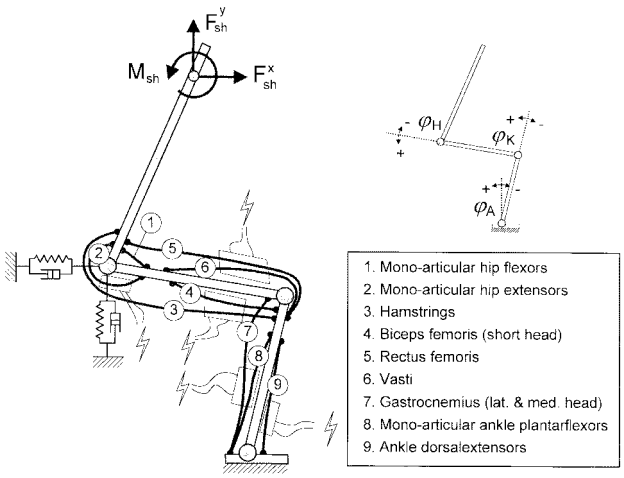

Fig. 1. Three segmental model with nine mono- and biarticular muscle groups. All muscle groups except monoarticular hip flexors (group 1) can be activated in experiment by the electrode arrangement used in this simulation study. The visco-elastic elements represent body-seat interaction. The two forces and one moment at the shoulder represent the control actions of the neurologically intact upper body.

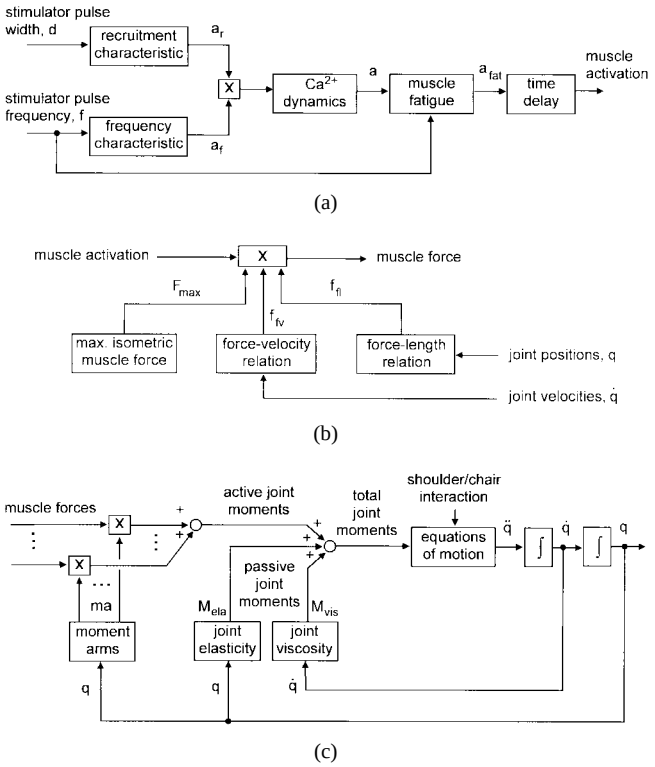

Fig. 2. The model of the stimulated plant comprises (a) an activation, (b) contraction, and (c) body-segmental dynamics part. Each muscle group has its own activation and contraction dynamics. The forces of the nine muscle groups are input to the body-segmental dynamics. The joint position vector is defined as $q = (\varphi_A, \varphi_K, \varphi_H)^T$.

described by a three-segmental model consisting of shanks, thighs, and upper body. Feet are flat on the ground. Nine mono- and biarticular muscle groups are modeled in the sagittal plane inducing moments about the ankle, knee, and hip joints (Fig. 1). It has to be noted, that one pair of electrodes may activate more than one muscle group depending on its position. Each group has its own activation and contraction dynamics. Input to each muscle group is the continuous time signal of the modulated pulse width and pulse frequency as provided by an electrical stimulator [see Fig. 2(a)]. Muscle activation is computed considering the effect of spatial and temporal summation by a nonlinear recruitment curve [6], a nonlinear activation-frequency relationship, and a linear second order calcium dynamics [7] (see Fig. 2(a) and Appendix I). A fatigue/recovery model [6] was incorporated which also takes into consideration that fatigue is increasing with rising stimulation frequencies. We implemented an additional constant time delay, $T_{\rm del}$, which is responsible for finite conduction velocities in the membrane system and delays from the chemical reactions involved. The active moment developed by a single muscle group is calculated from its nonlinear moment arm and the muscle force, which is a function of maximum isometric muscle force, muscle activation, force-length, and force-velocity relations (Fig. 2(b) and Appendix I).

In the body-segmental dynamics [see Fig. 2(c)] total joint moment is the sum of active, passive elastic, and passive viscous joint moments. Active joint moment is the sum of the joint moments produced by each muscle group (i.e., muscle force multiplied by moment arm). Passive muscle properties have been separated from the active muscle properties, and are assigned to the joints in order to keep the number of muscle parameters low. Passive elastic properties are modeled by double exponential equations which account for the influence of the adjacent joint angles (Appendix I and [8]). Passive viscous joint moments are modeled by linear damping functions (Appendix I). Equations of motion with three DOF describe the segmental dynamics of the body as well as the interaction with the environment (shoulder forces and seat interaction). Interaction with the seat is derived from [9]. A pair of nonlinear spring-dampers take into account the horizontal and vertical reaction forces (see Fig. 1 and Appendix I). The constraint requiring that vertical and horizontal seat reaction forces both have to be zero at seat-off is satisfied by introducing the effect of sliding between upper body and chair (Appendix I). The model is implemented in MATLAB/SIMULINK[1] and the computed motion is visualized by graphic animation. Model parameters are presented in Appendix II.

B. Modeling Voluntary Arm Support

Paraplegic patients need their arms during FES-supported movements not only to maintain balance but also to sustain the desired movement due to limited leg joint moments. Note that many patients are able to stand up even without the support of FES by arm support only using proprioceptive sensors of their upper body as well as vestibular and optical inputs to control the motion. Therefore, the upper body effort should be an integral part of any FES controller developed.

We assume that during open-loop and closed-loop standing up movements the patient tries to follow a trajectory he learned from past movements. For example, if the patient estimates his trunk position to be too far below its desired position at a specific instant of time, he will increase arm

[1] MATLAB/SIMULINK is a registered trademark.

TABLE I
FUZZY RULE SET FOR THE CONTROL OF HORIZONTAL SHOULDER POSITION

1.	**if**	Δx_{sh} is negative and big	**and**	$\dot{x}_{sh}$ is negative	**then**	F^x_{sh} is positive and big
2.	**if**	Δx_{sh} is negative and big	**and**	$\dot{x}_{sh}$ is zero	**then**	F^x_{sh} is positive and big
3.	**if**	Δx_{sh} is negative and big	**and**	$\dot{x}_{sh}$ is positive	**then**	F^x_{sh} is positive and big
4.	**if**	Δx_{sh} is negative and small	**and**	$\dot{x}_{sh}$ is negative	**then**	F^x_{sh} is positive and big
5.	**if**	Δx_{sh} is negative and small	**and**	$\dot{x}_{sh}$ is zero	**then**	F^x_{sh} is positive and small
6.	**if**	Δx_{sh} is negative and small	**and**	$\dot{x}_{sh}$ is positive	**then**	F^x_{sh} is negative and small
7.	**if**	Δx_{sh} is zero	**and**	$\dot{x}_{sh}$ is negative	**then**	F^x_{sh} is positive and small
8.	**if**	Δx_{sh} is zero	**and**	$\dot{x}_{sh}$ is zero	**then**	F^x_{sh} is zero
9.	**if**	Δx_{sh} is zero	**and**	$\dot{x}_{sh}$ is positive	**then**	F^x_{sh} is negative and small
10.	**if**	Δx_{sh} is positive and small	**and**	$\dot{x}_{sh}$ is negative	**then**	F^x_{sh} is positive and small
11.	**if**	Δx_{sh} is positive and small	**and**	$\dot{x}_{sh}$ is zero	**then**	F^x_{sh} is negative and small
12.	**if**	Δx_{sh} is positive and small	**and**	$\dot{x}_{sh}$ is positive	**then**	F^x_{sh} is negative and big
13.	**if**	Δx_{sh} is positive and big	**and**	$\dot{x}_{sh}$ is negative	**then**	F^x_{sh} is negative and big
14.	**if**	Δx_{sh} is positive and big	**and**	$\dot{x}_{sh}$ is zero	**then**	F^x_{sh} is negative and big
15.	if	Δx_{sh} is positive and big	**and**	$\dot{x}_{sh}$ is positive	**then**	F^x_{sh} is negative and big

force to lift his body and approach the desired position. Similarly, this also holds for horizontal deviations. Assuming this behavior we developed a simple tracking controller to model the patient's voluntary upper body effort. It modulates horizontal and vertical forces and a moment at the shoulder joint (Fig. 1) so that the shoulder follows a given reference trajectory as well as possible (force and moment values are limited). This controller is independent of the leg position, since there is no proprioceptive sensory information from the lower extremities being transmitted to the brain in complete lesions. The reference trajectory of the shoulder position and trunk inclination during the sit-to-stand transfer was obtained from an experiment with a paraplegic patient standing up with arm support only and no FES applied [10].

Three independent controllers are used to adjust horizontal and vertical shoulder forces and the shoulder moment as functions of $\Delta x_{\mathrm{sh}}, \Delta y_{\mathrm{sh}}, \Delta\varphi_{\mathrm{sh}}$ (deviations of horizontal and vertical shoulder joint position and trunk inclination from the desired values), and the velocities $\dot{x}_{\mathrm{sh}}, \dot{y}_{\mathrm{sh}}$, and $\dot{\varphi}_{\mathrm{sh}}$. Shoulder forces $(F^x_{\mathrm{sh}}, F^y_{\mathrm{sh}})$ and moments (M_{sh}) are calculated on the basis of a look-up table (control plane, see Fig. 3) that was determined by a procedure using the MATLAB[1] fuzzy control toolbox. Table I shows the rule set used to describe the control function of the horizontal shoulder position. The same rules were defined for vertical shoulder and trunk inclination control. Triangular membership functions were used to quantify the linguistic input and output variables (such as big, small, zero, etc.). By normalizing the input and output variables, a single control plane design could be used to adapt to each controller. The resulting arm controllers yield arm support that behave similar to a nonlinear elastic spring that connects the desired and actual shoulder joint position: the larger the distance between the actual and the desired shoulder position, the higher elastic forces will be produced to reduce this distance.

Fig. 4 shows the shoulder position and trunk inclination following the reference trajectory during simulation of a movement without the support of FES (arm support only).

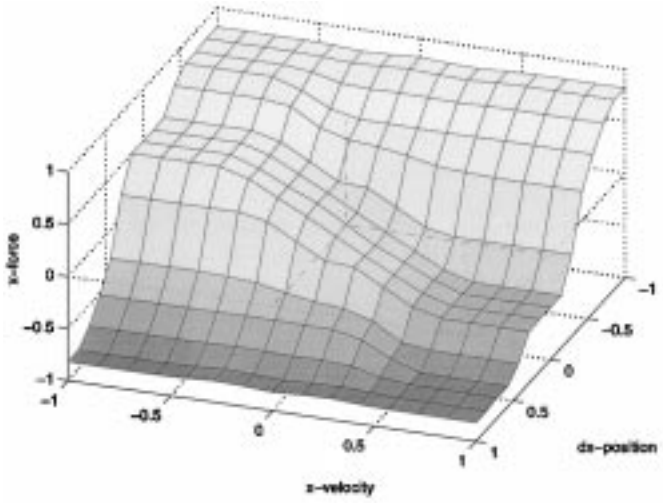

Fig. 3. Surface plot of the control function for the horizontal shoulder position. Inputs are the normalized horizontal shoulder position and velocity. Output is the normalized horizontal shoulder force. The same functions are used to calculated normalized vertical shoulder force and shoulder moment. Normalizing factors are used to determine the sensitivity of the controller toward input deviations and to adapt the shoulder force (controller output) to the strength of the simulated patient.

Comparison of simulated and measured standing-up movements show satisfactory agreement (Fig. 5).

C. Model Assumptions

In simulations stimulation is applied via five channels to each leg using surface electrodes. One pair of electrodes is attached to the buttocks, two pairs are attached to the thigh and another two to the shank as shown in Fig. 1. Note that the mono-articular hip flexor muscles (iliopsoas, group 1) are difficult to reach with surface electrodes, and therefore are not activated. Due to muscle atrophy in paralyzed limbs and insufficient muscle recruitment during artificial stimulation, paraplegics generate less muscle force than healthy subjects [10], [11]. In this study, we assume that the maximum

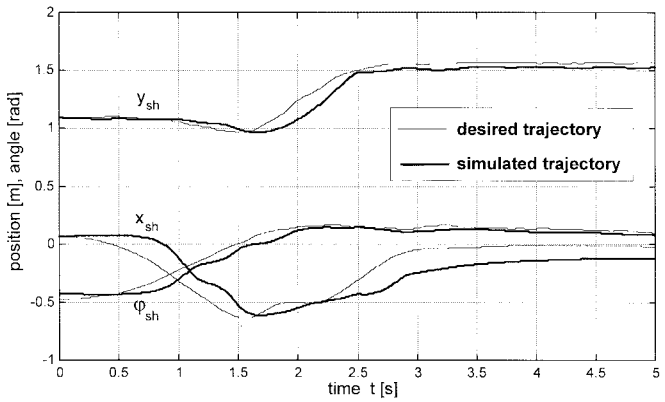

Fig. 4. Horizontal and vertical shoulder position ($x_{\rm sh}$, $y_{\rm sh}$, respectively) and trunk inclination ($\varphi_{\rm sh}$) of the desired and simulated standing-up movement without the support of FES (arm support only). The desired trajectory has been obtained from a paraplegic patient standing up without FES-support.

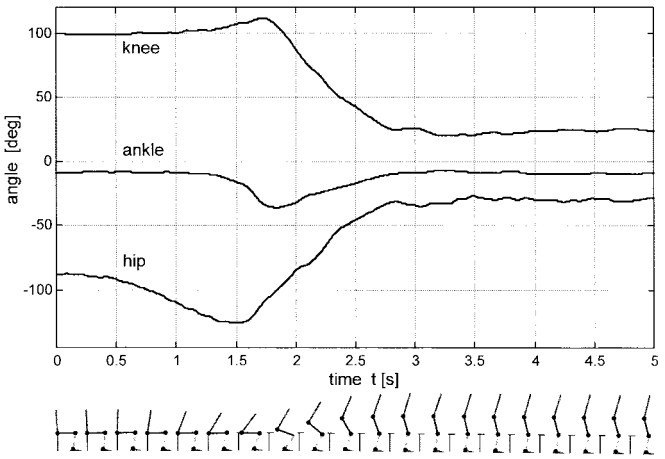

(a)

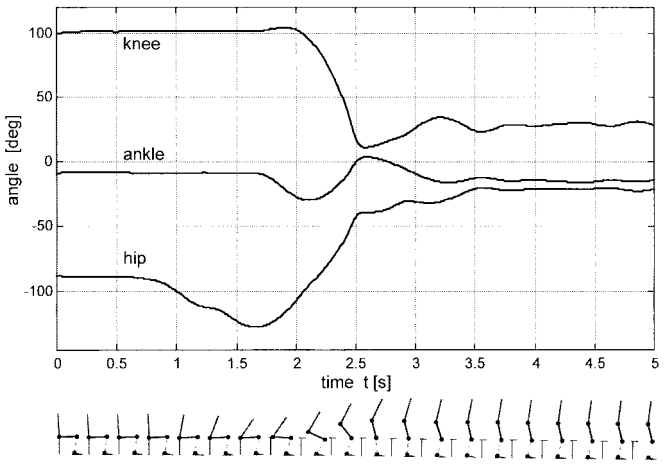

(b)

Fig. 5. (a) Standing-up movement without the support of FES (arm support only) in experiments and (b) in simulation. Notice that standing with the knee fully extended is not achieved. Complete extension of the knee can only be achieved when stimulating knee extensors as presented in the following figures. Satisfactory agreement is also obtained in the range of motion of ankle and hip.

paraplegic muscle force available is reduced to 45% of the maximum isometric muscle force produced by healthy subjects [12]. Shoulder force limitations during standing up were obtained from measurements performed by others [10], [13] ($|F^x_{\rm sh}| < 82$ N, $|F^y_{\rm sh}| < 330$ N, $|M| < 78$ Nm). Since we did not consider the foot explicitly in the model, additional computation of the center of pressure (COP) and friction allows observation of whether the foot intends to roll or slide, respectively (Appendix I).

D. Inverse Dynamic Model

An inverse dynamic version of the presented model was developed for implementation in the FES control strategy. Given the desired hip, knee, and ankle joint angles and their derivatives (angular velocities and accelerations), the inverse dynamic model estimates the stimulation pulse widths of each of the five channels employed to obtain the desired motion.

The inverse dynamic model was derived from the direct dynamic model of the patient presented in Appendix I. By inverting the equations of motion of the direct dynamic body-segmental model the total joint moments required to achieve the desired motion can be easily computed from the given joint kinematics. This procedure is called "computed torque," and is well known in the field of robotics [14]–[16]. Passive viscous and elastic joint moments are computed as presented in the direct dynamic model. The redundancy of five channels stimulating eight agonistic and antagonistic muscle groups which subsequently generate moments in three joints is solved by a linear optimization algorithm. It minimizes total muscle activation using a standard simplex algorithm as provided by the MATLAB optimization toolbox. Muscle moment arms as well as force-length and force-velocity factors are determined by (A12), (A6), and (A7), respectively. Some minor model simplifications were made. The nonobservable second-order calcium dynamics (PT_2) was inverted and low-passed to get a smooth estimate of the required motor unit activation (input to the forward calcium dynamics). The time delay as well as muscle fatigue are neglected in the inverse dynamic model. To get a unique solution for the stimulation pattern we assume a constant stimulation frequency ($f = 30$ Hz) while stimulation pulse width is modulated. The inverse recruitment curve is approximated by a piecewise linear function with a threshold, linear ramp, and saturation.

If it is not feasible to generate the muscle forces required to produce the desired motion (e.g., too high desired joint acceleration, or reduced maximum muscle forces due to atrophied muscle) the stimulation parameters are set to the maximum values. The ankle joint moment is truncated as soon as it exceeds values that violate the COP condition. If ankle moments were larger they would cause the foot to roll about the toes or heel (A14).

III. Implementation of Control Strategies

A. CHRELMS: Control by Handle Reactions of Leg Muscle Stimulation [5]

Donaldson and Yu state that many paraplegic patients can control the position and orientation of the trunk by voluntary

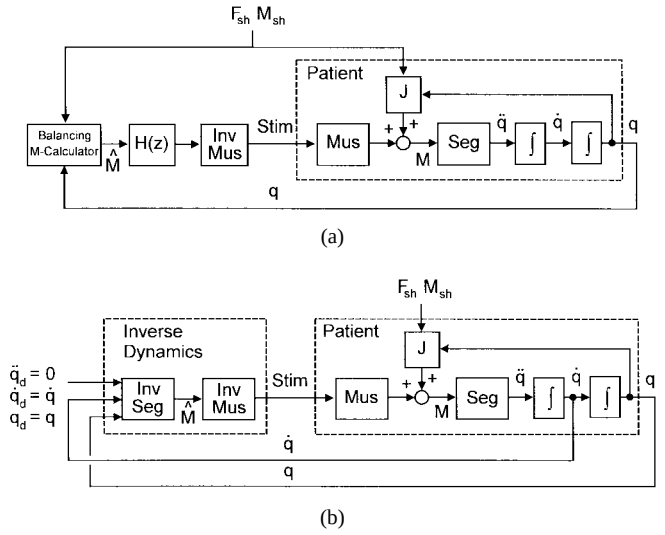

Fig. 6. Control strategies applied to the paraplegic patient model. (a) Structure derived from CHRELMS and (b) structure for PDMR. Mus: muscle activation and contraction dynamics model; Seg: segmental dynamics model including nonlinear moment arm computation; J: Jacobian matrix to map shoulder forces to joint moments; Inv Mus, Inv Seg: inverse of Mus and Seg, respectively; Contr: Controller; M, $\hat{M}$: actual and estimated joint moments, for $H(z) = 1.\mu\hat{M}$ is also called joint moment deficit [17]; Stim: pulse width of stimulation current; q, $\dot{q}$: joint angles and velocities, $q = (\varphi_A, \varphi_K, \varphi_H)^T$; $F_{\rm sh}$, $M_{\rm sh}$: shoulder forces and moment; $(\ )_d$: desired quantities.

upper body effort, and thus, the position of the two legs during FES-supported standing up [5]. The goal of the controller in their approach is to minimize handle reaction forces by mapping these forces to the equivalent leg joint moments and, as far as possible, adapt stimulation of the leg muscles to generate these moments. The key characteristic of this strategy compared to many other closed-loop strategies proposed in the FES literature is that no reference information, such as desired trajectory or path, is required.

We applied CHRELMS to the mathematical model of a paraplegic patient developed in this paper [see Fig. 6(a)]. The patient's movement is controlled by muscle stimulation and shoulder loads (i.e., forces and moments), which represent handle reaction loads. In this strategy the required leg joint moments $\hat{M}$ (called moment deficits in [17]) were estimated by a balancing moment calculator. A Jacobian matrix was used to obtain desired joint moments $\hat{M}$ from the actual shoulder forces and moments. The balancing moment calculator is followed by a discrete-time transfer function $H(z)$ (see [5, Fig. 4]). In this paper the transfer function used was $H(z) = 1$. An inverse dynamic muscle model was used to estimate the necessary stimulation pulse widths d from the required leg joint moments at a constant frequency f. In contrast to [5] our inverse model is dynamic, taking into account not only muscle recruitment but also muscle activation and contraction dynamics as described in Section II-D.

B. PDMR: Patient-Driven Motion Reinforcement

This strategy accounts for voluntary upper body effort as well, but does not require the recording of hand reactions. As in the CHRELMS algorithm, it is assumed that the patient provides sufficient arm force and is capable of controlling

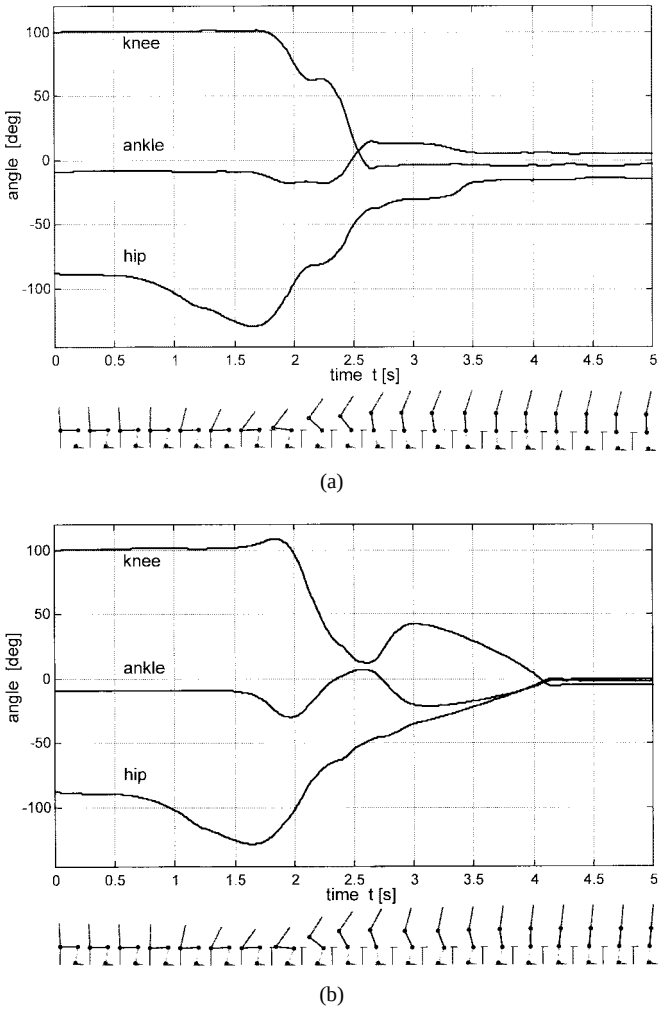

Fig. 7. (a) Simulated arm-supported movements generated by the CHRELMS and (b) by the PDMR. Shown are ankle, knee, and hip joint trajectories as well as stick figure drawings for the simulated patient during sit-to-stand transfer.

both the position and orientation of the trunk with his intact upper body. This allows many paraplegic patients to stand up even without the support of FES [10]. In this strategy the goal of reducing upper body effort is approached by presenting the controller with the movement initiated by the patient's voluntary effort. Actual joint positions and velocities are fed back into the inverse dynamic model, which predicts the stimulation pulse widths required to maintain the movement. This controller structure is shown in Fig. 6(b). The desired angular joint accelerations input to the inverse model are always set to zero, and so changes in motion are left to the patient. The FES pattern adapts to the voluntary movement the patient initiates and—as with CHRELMS—no reference trajectory or path is required.

IV. Results

A. Results with the CHRELMS Strategy

With CHRELMS hip and knee joints extend synchronously while the angle of the ankle joint almost remains constant during early rising phase [see Fig. 7(a)]. However, later in the

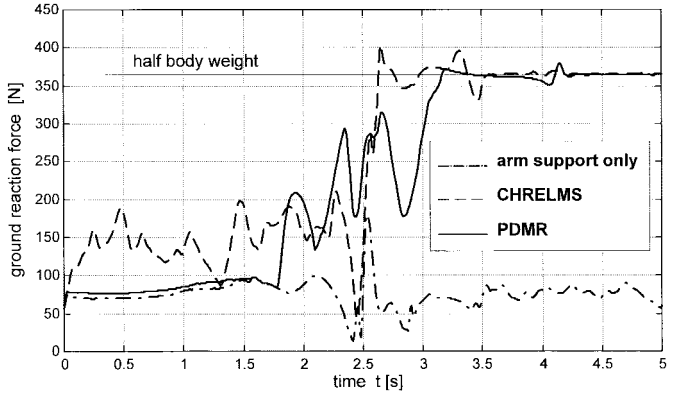

(a)

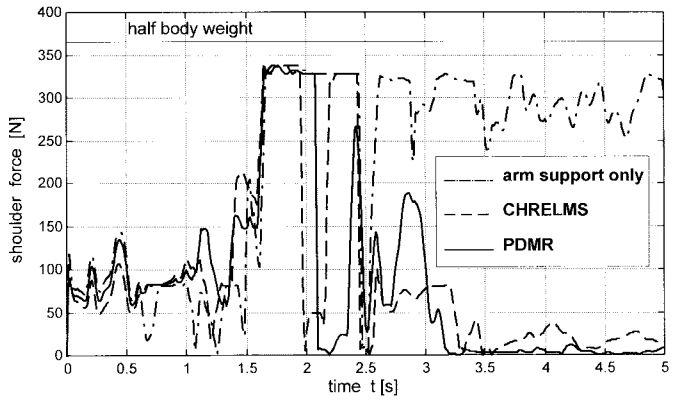

(b)

Fig. 8. (a) Ground reaction forces and (b) shoulder forces for simulation results with arm support only (dash-dotted line), with CHRELMS (dashed line), and with PDMR (continuous line) for one side of the body. Half body weight is indicated by a thin straight line. Absolute force values result from the vector sum of horizontal and vertical ground reaction forces. Note that with arm support only (no FES), the full body weight does not have to be carried by the arms since the feet touch the ground and thus transfer part of leg weight through the ground.

rising phase the ankle joint suddenly enters plantarflexion. At the beginning of rising the legs carry only a small portion of the body weight [see Fig. 8(a)]. During late rising phase and standing, this value quickly increases to 100% [see Fig. 8(a)], thus reducing arm forces significantly [see Fig. 8(b)].

During standing only the knee joint is fully extended. Hip and ankle joint do not reach full extension within the plotted time-interval, but standing posture is improved, compared to the movements without FES-support (Fig. 5). A reason for the incompletely erected standing posture in CHRELMS might be that the arm model of upper body effort used in the present simulation study is not sufficient for this strategy (see Section V-A). Unlike the vertical and horizontal shoulder position, trunk inclination does not reach the desired value of the arm controller. The shoulder moment resulting from the trunk inclination error is too small to move the trunk into a fully upright position. However, the three leg joints are in full alignment during standing as the knee is fully extended [see Fig. 7(a)]. This posture could be achieved, although—in a quasistatic analysis—the upper body cannot control leg joint moments when hip, knee, and ankle are exactly aligned [5]. As already stated by Donaldson and Yu [5], a quasistatic analysis

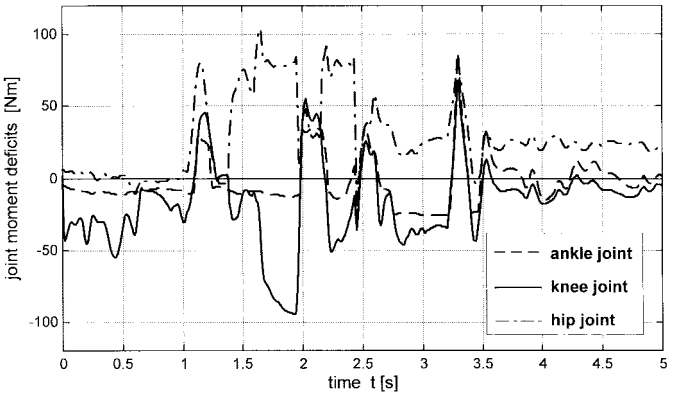

Fig. 9. Moment deficits $\hat{M}$ in ankle, knee, and hip joint to reduce upper body effort in the CHRELMS simulation. Values are computed by the balancing moment calculator (Fig. 6) from shoulder forces and moments. The hip joint moment deficit is positive, causing FES-induced hip extension as desired to stand up. The knee joint moment deficit is mostly negative, causing knee extension which is also desired. It can be seen that when the knee moment deficit becomes positive at $t = 1.95$ s (thus, a flexion moment is generated) the knee slightly flexes until the shoulder position error is large enough to produce a corrective arm effort [see Fig. 7(a)].

does not hold close to full extension. Yet, the case mentioned is dynamic: the knee moves rapidly from flexion through extension to hyperextension, thus, overcoming the singularity at full extension.

In simulations with $H(z) = 1$, sudden changes of arm forces and moments promptly appear in the required stimulator output due to the structure of the system [Fig. 6(a)]. Since arm actions directly influence the stimulation pattern rapid changes in the recorded arm reactions due to balance keeping reactions, muscle trembling in the arms or other disturbances, also appear in the stimulation pattern and affect the resulting movement. Depending on the direction of the arm force vector the required joint moments could impede the desired movement (e.g., force vector in front of the knee leads to undesired knee flexion moments during standing up). This is in accordance with observations in experiments performed by Donaldson and Yu [17]. In the CHRELMS simulation the required joint moments are mainly knee and hip extension moments (Fig. 9) resulting in a successful standing-up movement.

Using a different $H(z)$ might overcome the disadvantages mentioned above. However, when we tried $H(z)$ as an integrator, as proposed in [5] for the static case, a natural standing-up movement could not be achieved. Leg muscles cannot provide sufficient force to realize standing up, thus arm forces are always positive (to support the legs), and cause integrator wind up. This significantly hampers the resulting movement.

B. Results with the PDMR Strategy

With our PDMR strategy both the hip and knee joints show fast and smooth extension movements during the early rising phase [see Fig. 7(b)] as has been observed with the CHRELMS strategy. However, as soon as the knee has reached almost full extension, it suddenly buckles by about 25°, and the ankle joint goes back into the desired dorsiflexion. After this interruption, knee and ankle extension continues and finally the body reaches an upright position. This increases the duration of the sit-to-stand transfer for more than one

second compared to CHRELMS. The buckling of the knee joint is due to insufficient lower leg muscle forces and a temporary reduction of vertical arm forces induced by the arm controller (see Figs. 7(b) and 8(b) at $t = 2.2 \cdots 2.7$ s). A similar, although less significant effect is observed with CHRELMS (see Figs. 7(a) and 8(b) at $t = 1.95$ s). With insufficient muscle forces the knee moment deficit becomes positive (see Fig. 9), i.e., the knee produces a flexion moment at $t = 1.95$ s. The knee slightly flexes until the shoulder position error is large enough to produce a corrective arm effort. In simulations where muscle forces of a neurologically intact subject are assumed (100% maximum muscle forces, $F_{\max}$, Appendix II, Table II), this effect was not observed. Although the buckling behavior of the arm controller is not desired, it has no adverse effect on the overall movement. It rather improves posture by moving the hip position in front of the ankle joint. In the PDMR strategy standing is achieved with the hip, knee, and ankle joints approximately aligned. The reduction of arm forces in the PDMR strategy is higher than in the CHRELMS strategy. During rising $(t = 2.2 \cdots 3.0$ s) the legs carry more than 50% of the body weight (see Fig. 8). During standing this value increases to 100%.

In this strategy the voluntary upper-body contribution of the patient is presented indirectly to the controller in terms of resulting joint angles and angular velocities. Since joint angles and velocities are first and second order responses, respectively, the voluntary upper body effort is reflected in a low-passed manner [see integrating blocks in Fig. 6(b)]. As joint angles and velocities are the values used to estimate the required stimulator output, increased robustness and stability are obtained with respect to arm disturbances or trembling. Of course, appropriate sensor systems are necessary to achieve this goal. However, since joint velocities are fed back, this strategy also reinforces patient movement during standing. To prevent instability, we recommend setting $\dot{q}_d$ equal to zero [see Fig. 6(b)] or switching to another control strategy during standing.

V. Discussion

The CHRELMS strategy proposed by Donaldson and Yu [5] and the PDMR strategy presented in this study show similar results (see Figs. 7 and 8). Both strategies significantly improve movements as compared to standing up without FES-support (arm support only, Fig. 5) or open-loop FES-support [10]. During early rising phase with PDMR, the legs carry a significant portion of the body weight; during late rising phase and standing, in both strategies this value increases to 100% [Fig. 8(a)]. Thus, both strategies lead to a significant reduction of arm forces [see Fig. 8(b)]. Furthermore, hip, knee, and ankle joint achieved improved alignment for the standing phase in both strategies. Note that the joint angle trajectories of both strategies are comparable with trajectories recorded in healthy subjects [10], although no reference data, such as joint trajectories, is required by the controller.

A. Importance of Considering Voluntary Upper Body Support

Many other approaches which focus on FES-supported movements in paraplegics neglect the influence of the voluntary upper body or simply consider it as a disturbance being subject to compensation [18]–[22]. Veltink [23] proposed an interesting strategy, in which arm support is considered as a perturbation of the system. In this strategy a controller first calculates the joint moments required to realize a desired movement without considering arm support. Subsequently, these values are reduced by the moments resulting from upper body effort. The remaining moment is then generated by the stimulated muscle groups. This approach is well known in the control theory literature, and is often referred to as disturbance compensation or disturbance decoupling [24]. However, it is unclear if disturbance compensation of upper body effort is feasible in view of the nonlinear and time-delayed properties of the human body.

It appears that it is important to include voluntary upper body effort in the design of closed-loop controllers for paraplegic patients. If arm support is considered as a disturbance which has to be compensated for, the controller is likely to hamper the indispensable effort of the patient. Moreover, artificial and natural control could adversely interfere, resulting in undesired or even dangerous motion and increased arm forces. With both CHRELMS and PDMR, as shown in this study, upper body effort can be advantageously utilized to allow a patient to drive the entire system dynamics. Thus, the system can benefit from the patient's ability to better adapt and learn than technical controllers do.

The model of upper body effort presented here is thought to be a first step toward including voluntary effort into physiological modeling and simulation. If it is desired to develop patient-driven controllers based on simulations, it is crucial that the model used reflects to some degree the patient's voluntary behavior. We do not claim to model the patient's free will, but with this model it is at least possible to have a patient stand up with the support of his arms, or independently without FES while being capable of responding to external disturbances. The performance of the shoulder controller is limited by the fact that it tries to follow a fixed time course. As a first improvement, it is planned to avoid shoulder reference trajectories as functions of time to obtain a more flexible response to external disturbances.

B. Does the Inverse Dynamic Model "Cancel" the Plant?

The application of linear control strategies to highly nonlinear systems such as complex physiological systems is not optimal, especially if the controller has to operate within a wide dynamic range. Nonlinear control theory provides an approach based on inverse modeling in which required input values are calculated from the desired output. The main goal of implementing an inverse model is to compensate for the nonlinearities of the plant [25]. The more accurate and realistic the inverse dynamic model, the closer to reality is the feedforward prediction of the required stimulation pattern, thus, the smaller is the error to be corrected by a feedback controller. One could say that an ideal inverse dynamic model would "cancel" the plant. Prediction of joint moments by an inverse dynamic model is well known in robotics (computed torque, [14]–[16]). In the control of FES-induced single joint

movements the use of an inverse dynamic model has shown to be a promising strategy for controlling joint angle [25], [26].

Inverse dynamic models are only satisfactorily if the plant is well identified. In an experimental setup this requires very careful parameter identification procedures to adapt the inverse dynamic model to the individual subject. Moreover, not every system can be inverted, and approximations are required in these cases. Although the inverse dynamic model will never be exact, we suggest that a controller design based on approximated inverse dynamic models will still significantly improve the controller performance as compared to commonly used linear (e.g., PID) controllers.

In the present study the inverse dynamic model is calculated from the direct dynamic model of the simulated plant. Therefore, it is capable of predicting the required stimulation pattern from the desired joint motion, while compensating partially for the nonlinearities of the system. However, prediction of the inverse model presented in this study is not exact for the following reasons: 1) the time delay T_{del} cannot be canceled, 2) input constraints of the plant (force limitations of artificially stimulated paralyzed muscle) and truncated ankle joint moments in case of COP violations may result in insufficient stimulator output, and 3) minor model simplifications were required to obtain an inverse dynamic model of the muscle recruitment/activation dynamics (see Section II-A). Thus, an ideal cancellation of the plant even in the simulation is not possible, although desired to improve the control performance.

Due to undesirable parasitic effects such as nonideal cancellation, erroneous estimation of inverse dynamic model parameters, changes in system behavior due to fatigue, external or internal disturbances such as spasticity or interaction with the environment, cancellation needs to be "robustified," for example, with a feedback controller [25], [26]. In our PDMR approach, and this is the most novel element of the work presented here, the patient drives the FES-supported standing-up motion by his or her upper body effort. Thus, errors in the prediction of the required stimulation parameters will be corrected by the actions of the arms, so that the patient compensates the parasitic effects mentioned above. Thus, the patient is the feedback controller who is "robustifying" the cancellation strategy.

In reality the inverse dynamic model is fed with noisy sensor signals. Since the physical plant acts as a low pass filter, there is a danger that the inverse will amplify this measurement noise, thus, yielding nonoptimal muscle stimulation. The design of an additional inner-loop controller could improve the controller performance and simplify the human's task.

C. Stability and Robustness

In this study, the stability and robustness of the control strategies are difficult to prove using classical control theory. However, in simulations no unstable situation occured. The main reason is that the influence of the arms is quite strong compared to the force produced by stimulation of the lower extremities. Arm effort is an intrinsic part of the system and cannot be considered as simple disturbances. Furthermore, in the model the forces at the shoulder generated to control the upper body movement act considerably faster than the stimulated muscles of the lower extremities (time delay, damped system). It can be assumed that errors in the stimulation of the lower extremities can, to some extent, be corrected by the arms. Although this may interfere with a significant reduction of supporting arm forces, a safe standing-up motion is expected independently of the applied stimulation pattern as in Fig. 5.

To at least obtain some qualitative information about the robustness of the two strategies, sensor noise and parameter errors (10–30%) of the inverse dynamic model were implemented. Whereas poor sensory signals strongly decrease the quality of the movements, in the presence of inverse dynamic parameter uncertainties the resulting standing-up movements were still satisfactory. Reduction of upper body effort was significant although less effective as the erroneous inverse dynamic model parameters lead to an incorrect prediction of the stimulation pattern. It was observed that different strategies (closed-loop compared to open-loop) become less distinct with increasing model uncertainties. This supports our assertion that the arms are dominant over the artificially controlled and stimulated lower body. To better assess the differences we therefore neglected sensor noise and parameter errors in the present study.

In further simulations we also replaced some of the anthropometric and muscle parameters of the direct dynamic model by another parameter set in order to test the controller performance for a different individual. In comparison to the previous simulation runs the resulting standing-up movements did not change significantly.

VI. Conclusion

A mathematical model that describes relevant properties of stimulated muscles and resulting segmental movements was presented. Two strategies, the CHRELMS strategy [5] and the PDMR strategy developed here, were tested for standing-up movements by applying them to the model. Compared to classical FES closed-loop approaches, neither strategy requires a predetermined reference input for the leg joints (e.g., desired trajectories). The generation of moments in the paralyzed limbs and, thus, the standing-up movement is driven by the patient's voluntary upper body effort, rather than imposing a preprogrammed reference trajectory on the patient. Furthermore, the legs carry a higher amount of the body weight so that the arm forces required were significantly lower than in movements without stimulation.

The model presented in Section II-A and Appendix I was not only used to validate the two strategies. Although not shown in this paper, it already contributed to the development of the PDMR strategy in a significant manner. Time-consuming and perhaps troublesome trial-and-error experimentation can be avoided or at least shortened and the number of experiments in humans can be reduced. Both of which will accelerate the development of neural prostheses.

It should be noted that the two strategies were only tested with a few specific models each, comprising a specific choice of parameters, sensors, and electrode arrangement. Therefore, we do not claim that the results presented in this paper can

be generalized. A modified model of the simulated patient or changes to the control strategies may lead to different results. Similarly, disturbances such as spasticity, sensor noise, and measurement errors will significantly affect the quality of the different control strategies under real life conditions. Therefore, experimental studies have to be performed to eventually validate the developed strategies on several patients with different muscle properties and anthropometry.

APPENDIX I
MODEL EQUATIONS

The normalized portion of motor units recruited, a_r ($0 \leq a_r \leq 1$), is calculated as a function of the pulse width d (Fig. 2: recruitment characteristic), using following equation [6]:

$$a_r(d) = c_1\{(d-d_{\text{thr}})\arctan[\kappa_{\text{thr}}(d-d_{\text{thr}})] - (d-d_{\text{sat}})\arctan[\kappa_{\text{sat}}(d-d_{\text{sat}})]\} + c_2 \quad \text{(A1)}$$

where d_{thr} and d_{sat} denote pulse width values corresponding to threshold and saturation, respectively. The curvatures of the recruitment curve in the area of threshold and saturation can be adjusted by changing κ_{thr} and κ_{sat}, respectively. The recruitment curve is scaled by the constants c_1 and c_2 in order to satisfy the conditions $a_r(0) = 0$ and $a_r(d) \to 1$ for $d \to \infty$.

The normalized amount of activation a_f ($0 \leq a_f \leq 1$) in a single motor unit is expressed as a function of stimulation frequency f (Fig. 2)

$$a_f(f) = \frac{(\alpha f)^2}{1+(\alpha f)^2} \quad \text{(A2)}$$

where α is a shape factor. This function has been introduced by the authors and captures the force-frequency characteristic of an artificially stimulated muscle.

The calcium Ca^{2+} dynamics has been modeled by two first order transfer functions in series (time constant T_{Ca}). Input into the calcium dynamics model is the product of a_r and a_f, while the output is the activation a of a nonfatiguing muscle (see Fig. 2).

To describe the effect of muscle fatigue we introduced a fitness function $fit(t)$, modified from [6], which can be expressed by the following first-order relation:

$$\frac{dfit}{dt} = \frac{(fit_{\min}-fit)a\lambda(f)}{T_{\text{fat}}} + \frac{(1-fit)(1-a\lambda(f))}{T_{\text{rec}}} \quad \text{(A3)}$$

$$\lambda(f) = 1-\beta+\beta\left(\frac{f}{100}\right)^2 \quad \text{for} \quad f < 100 \text{ Hz}. \quad \text{(A4)}$$

The minimum fitness is given by $fit_{\min}$. The time constants for fatigue T_{fat}, and recovery T_{rec}, can be estimated from stimulation experiments [6]. The term $\lambda(f)$ in (A3) and (A4) is a function of stimulation frequency, while β is a shape factor. $\lambda(f)$ has been introduced by the authors to better account for the fact that muscle fatigue rate strongly depends on stimulation frequency. Finally, the activation of fatiguing muscle is given by

$$a_{\text{fat}}(t) = a(t)fit(t). \quad \text{(A5)}$$

In the muscle contraction dynamics the muscle activation as computed by (A1)–(A5) is scaled by the maximum isometric muscle force, and the factors f_{fl} and f_{fv} describing the force-length and force-velocity relation, respectively, in order to get the absolute muscle force (Fig. 2).

The force-length relation is given by [27]

$$f_{\text{fl}} = \exp\left[-\left(\frac{\bar{l}-1}{\varepsilon}\right)^2\right] \quad \text{(A6)}$$

where $\bar{l}$ is the muscle length normalized with respect to the optimal muscle length l_{opt} and ε is a shape factor. The force-velocity relation can be described as follows [28]:

$$f_{\text{fv}} = 0.54\arctan(5.69\bar{v}+0.51)+0.745 \quad \text{(A7)}$$

where $\bar{v}$ is the muscle velocity normalized with respect to the maximum contraction velocity v_m of the muscle ($\bar{v} = v/|v_m|$, where $v = dl/dt$ and $v < 0$ for muscle contraction).

Muscle length l_i and velocity v_i of muscle group i are determined by the position φ_j and the velocity $\dot{\varphi}_j$ of the joints j which the muscle spans:

$$l_i = C_i + \sum_j \int_{\varphi_j} ma_{ij}(\varphi_j)\,d\varphi_j \quad \text{(A8)}$$

$$v_i = \sum_j \dot{\varphi}_j ma_{ij}(\varphi_j). \quad \text{(A9)}$$

In these equations ma_{ij} is the moment arm of muscle group i around joint j. C_i is an integration constant resulting from integration of the moment arm functions. Equations (A8) and (A9) have been derived assuming that the moment arm is the derivative of the muscle length with respect to joint angle ($ma_{ij} = dl_i/d\varphi_j$). Moment arms were represented as algebraic functions of joint angles that have been fitted to measured moment arm curves from the literature (hip joint [29]–[31], knee joint [31]–[35], and ankle joint [36]–[38]). The moment arm curve of the entire muscle group was obtained by the weighted averaging (with respect to maximum muscle force) of the moment arm curves for the single muscles in the group.

The moment arms ma_{ij} of muscle groups $i = 1 \cdots 9$ (see Fig. 2) at the hip, knee, and ankle joint are described as follows:

$$\begin{aligned}
\text{hip joint:} \quad & ma_{1H} = 0.00233\varphi_H^2 - 0.00223\varphi_H - 0.0275 \\
& ma_{2H} = -0.0098\varphi_H^2 - 0.0054\varphi_H + 0.0413 \\
& ma_{3H} = -0.020\varphi_H^2 - 0.024\varphi_H + 0.055 \\
& ma_{5H} = 0.025\varphi_H^2 + 0.41\varphi_H - 0.040 \\
\text{knee joint:} \quad & ma_{3K} = -0.0098\varphi_K^2 + 0.021\varphi_K + 0.028 \\
& ma_{4k} = -0.008\varphi_K^2 + 0.027\varphi_K + 0.014 \\
& ma_{5K} = -0.058\exp(-2.0\varphi_K^2)\sin\varphi_K - 0.0284 \\
& ma_{6K} = -0.070\exp(-2.0\varphi_K^2)\sin\varphi_K - 0.0250 \\
& ma_{7K} = 0.018 \\
\text{ankle joint:} \quad & ma_{7A} = 0.053 \\
& ma_{8A} = 0.035 \\
& ma_{9A} = 0.013\varphi_A - 0.035. \quad \text{(A10)}
\end{aligned}$$

The passive viscous moment of joint j has been modeled as a linear relation between the angular joint velocity $\dot{\varphi}_j$ and the damping coefficient k_j:

$$M_{\text{vis},j} = k_j \dot{\varphi}_j \tag{A11}$$

Passive elastic joint moments $M_{\text{ela},j}$ are [8]

$$\begin{aligned}
\text{ankle joint:}\quad M_{\text{ela},A} &= \exp(2.0111 - 0.0833\varphi_A \\
&\quad - 0.0090\varphi_K) \\
&\quad - \exp(-9.9250 + 0.2132\varphi_A) \\
&\quad - 2.970 \\
\text{knee joint:}\quad M_{\text{ela},K} &= \exp(1.0372 + 0.0040\varphi_A \\
&\quad - 0.0494\varphi_K - 0.0250\varphi_H) \\
&\quad - \exp(-1.1561 - 0.0020\varphi_A \\
&\quad + 0.0254\varphi_K + 0.0030\varphi_H) \\
&\quad + \exp(2.5 - 0.25\varphi_K) + 1.0 \\
\text{hip joint:}\quad M_{\text{ela},H} &= \exp(2.1080 - 0.0160\varphi_K \\
&\quad - 0.0195\varphi_H) \\
&\quad - \exp(-2.1784 + 0.070\varphi_K \\
&\quad + 0.1349\varphi_H) - 15.24.
\end{aligned} \tag{A12}$$

In (A10)–(A12) angles are in degrees. Positive values produce hip extension, knee flexion, and ankle plantarflexion as shown in Fig. 1.

The interaction with the chair was modeled by a horizontal and vertical spring-dashpot element with nonlinear properties as presented by Pandy *et al.* [9]. However, to fulfill the condition that elastic and damping contact force are zero at seat-off Pandy's equation for $\Delta y < 0$ was modified to

$$\begin{aligned}
F^x_{\text{ela}} &= -\text{sign}(\Delta x) 500N(10^{60|\Delta x|} - 1) \\
F^x_{\text{dam}} &= -2500N\dot{x}[1 - \exp(-1000|\Delta y|)] \\
F^y_{\text{ela}} &= 50N(10^{60|\Delta y|} - 1) \\
F^y_{\text{dam}} &= -2500N\dot{y}[1 - \exp(-1000|\Delta y|)]
\end{aligned} \tag{A13}$$

where Δx and Δy are the horizontal and vertical displacement between hip and seat, respectively. F_{ela} is the elastic force and F_{dam} the damping force between seat and body. To ensure that both the horizontal and the vertical components of the seat force reduce to zero simultaneously at the instant of seat lift-off, the hip was permitted to slide in the horizontal direction if the magnitude of the horizontal component of force was greater than the product of the magnitude of the vertical component of force and the coefficient of friction μ_{cli} ($\mu_{\text{cli}} = 1$ in this study, more details in [9]).

To avoid the foot rolling about the toes or the heel the center of pressure has to remain below the supporting area of the foot. Thus, assuming a massless foot attached to the ground the total ankle joint moment M_A has to fulfill the following condition:

$$F^y_{\text{gr}}\Delta x_{\text{heel}} - F^x_{\text{gr}}\Delta y < M_A < F^y_{\text{gr}}\Delta x_{\text{toes}} + F^x_{\text{gr}}\Delta y \tag{A14}$$

where F^x_{gr} and F^y_{gr} are the horizontal and vertical ground reaction forces, respectively, Δx_{heel} is the horizontal distance between ankle joint and heel, Δx_{toes} is the horizontal distance between ankle joint and toes, and Δy is the vertical distance between ankle joint and ground.

To avoid sliding of the foot the following condition has to be fulfilled:

$$F^x_{\text{gr}} < \mu_{\text{gr}} F^y_{\text{gr}} \tag{A15}$$

where F^x_{gr} is the horizontal ground reaction force and μ_{gr} is the friction coefficient for the feet on the ground.

TABLE II
MUSCLE-SPECIFIC PARAMETERS OF THE ACTIVATION AND CONTRACTION DYNAMICS MODEL: T_{Ca} IS THE TIME CONSTANT OF THE SECOND-ORDER CALCIUM DYNAMICS, T_{fat} IS THE FATIGUE TIME CONSTANT, $\text{fit}_{\min}$ IS THE MINIMUM MUSCLE FITNESS, $F_{\max}$ IS THE MAXIMUM ISOMETRIC MUSCLE FORCE, l_{opt} IS THE OPTIMAL MUSCLE LENGTH, C_i IS THE MUSCLE LENGTH CONSTANT, ε IS THE SHAPE FACTOR OF THE FORCE-LENGTH RELATION, AND v_m IS THE MAXIMUM CONTRACTION VELOCITY

Muscle group	T_{Ca} [s]	T_{fat} [s]	fit_{min}	F_{max} [N] (100%)	l_{opt} [m]	C_i [m]	ε	v_m [m/s]
1	0.04	18	0	1850	0.146	0.165	0.4	0.73
2	0.04	18	0	2370	0.11	0.05	0.5	0.54
3	0.05	25	0.2	2190	0.121	0.09	0.4	0.48
4	0.05	25	0.2	400	0.173	0.18	0.2	0.69
5	0.03	18	0	1000	0.086	0.11	0.4	0.51
6	0.04	18	0	5200	0.086	0.04	0.45	0.48
7	0.05	18	0	1600	0.054	0.06	0.3	0.32
8	0.07	40	0.5	3600	0.033	0.028	0.5	0.1
9	0.06	33	0.3	1100	0.099	0.09	0.4	0.36

APPENDIX II
MODEL IDENTIFICATION

Muscle-specific parameters were derived from the literature [12], [39]–[47], (Table II). In a first step the average percentage of fast and slow motor units in the nine muscle groups was determined using data from Johnson *et al.* [39]. Then, muscle properties that depend on the fiber composition of the muscle, e.g., the fatigue and contraction behaviors, were identified. Fatigue parameters (T_{fat} and $fit_{\min}$) were determined so that slow muscle groups (such as group 8 which is comprised of mainly soleus muscle) showed a more fatigue-resistant behavior than the fast muscle groups [40]. Similarly, the time constants T_{Ca} for the Ca^{2+} dynamics were adjusted so that the contraction behavior for the different muscle groups corresponded well with data given in the literature [41], [42]. The T_{Ca} values chosen in this model yield contraction times between 50 ms (muscle group 5: mainly rectus femoris muscle) and 90 ms (muscle group 8: mainly soleus muscle). The maximum contraction velocities v_m were calculated from the percentage of fast muscle fibers and the optimum muscle length on the basis of an estimate given in [43]

$$\begin{aligned}
\text{slow muscle fibers: } v_m &= 2l_{\text{opt}}\tfrac{1}{s} \\
\text{fast muscle fibers: } v_m &= 8l_{\text{opt}}\tfrac{1}{s}.
\end{aligned} \tag{A16}$$

Maximum isometric muscle force $F_{\max}$ and optimal muscle lengths l_{opt} of the muscle groups were taken from Delp [12] by averaging the values provided for single muscles. Note that to model the musculoskeletal system of a paraplegic patient $F_{\max}$ has been reduced to 0.45 $F_{\max}$. The parameters C_i and ε required to describe the force-length relation were adjusted so that simulated and measured maximum voluntary joint moments versus joint angle [12] showed good agreement.

TABLE III
MUSCLE-INDEPENDENT MODEL PARAMETERS: $d_{\rm thr}$, $d_{\rm sat}$ ARE RECRUITMENT THRESHOLD AND SATURATION, RESPECTIVELY, α IS THE FORCE-FREQUENCY SHAPE FACTOR, β IS THE FATIGUE-FREQUENCY SHAPE FACTOR, $T_{\rm rec}$ IS THE RECOVERY TIME CONSTANT, $T_{\rm del}$ IS THE TIME DELAY, AND k_A, k_K, AND k_H ARE THE DAMPING COEFFICIENTS IN ANKLE, KNEE, AND HIP JOINT, RESPECTIVELY

$d_{\rm thr}$ [μs]	$d_{\rm sat}$ [μs]	α [s]	β	$T_{\rm rec}$ [s]	$T_{\rm del}$ [s]	k_A, k_K, k_H [Nms/rad]
122.0	487.0	0.1	0.6	30	0.025	0.6 1.0 2.0

TABLE IV
ANTHROPOMETRIC DATA OF SHANK, THIGH, AND HAT (HEAD, ARMS, AND TRUNK)

	length [m]	center of gravity [m]	mass (half body) [kg]	moment of inertia (half body) [kg m^2]
shank	0.45	0.279	3.5	0.0476
thigh	0.50	0.244	10.0	0.2431
HAT	0.80	0.469	23.7	2.6967

Muscle-independent model parameters are presented in Table III. No satisfactory data could be found in the literature which allows different muscle groups to be sufficiently distinguished. $d_{\rm thr}$ and $d_{\rm sat}$ were taken from [6]. α and β were adjusted so that simulated fatigue curves corresponded well to data presented in [44] and [45], respectively. The choice for $T_{\rm del} = 0.025$ s is discussed in detail in [46]. The knee damping coefficient k_K was adjusted so that experimental and simulated pendulum tests of the shank showed good agreement [6]. k_A and k_H were roughly estimated from k_K taking into account the amount of muscle mass surrounding the respective joint. Anthropometric parameters (Table IV) were estimated on the basis of regression equations as provided in [47].

ACKNOWLEDGMENT

The authors are indebted to Dr. S. J. Dorgan for his support during this study. Furthermore, they want to thank Prof. G. Schmidt, Dr. J. Quintern, F. Bahrami, and Dr. M. Buss for their advice.

REFERENCES

[1] A. Kralj and T. Bajd, *Functional Electrical Stimulation*. New York: CRC Press, 1989.
[2] R. J. Jaeger, "Lower extremity applications of functional neuromuscular stimulation," *Assistive Technol.*, vol. 4, pp. 19–30, 1992.
[3] H. M. Franken, P. H. Veltink, and H. K. B. Boom, "Restoring gait in paraplegics by functional electrical stimulation," *IEEE Eng. Med. Biol.*, vol. 13, pp. 564–570, 1994.
[4] E. B. Marsolais and R. Kobetic, "Functional electrical stimulation for walking in paraplegia," *J. Bone Joint Surg.*, vol. 69-A, pp. 728–733, 1987.
[5] N. de N. Donaldson and C. H. Yu, "FES standing control by handle reactions of leg muscle stimulation (CHRELMS)," *IEEE Trans. Rehab. Eng.*, vol. 4, pp. 280–284, 1996.
[6] R. Riener, J. Quintern, and G. Schmidt, "Biomechanical model of the human knee evaluated by neuromuscular stimulation," *J. Biomechan.*, vol. 29, pp. 1157–1167, 1996.
[7] H. Hatze, "A general myocybernetic control model of skeletal muscle," *Biol. Cybern.*, vol. 28, pp. 143–157, 1978.
[8] R. Riener and T. Edrich, "Significance of passive elastic joint moments in FES," in *Proc. 2nd IFESS Conf.*, Vancouver, B.C., Canada, Aug. 1997, pp. 103–106.
[9] M. G. Pandy, B. A. Garner, and F. C. Anderson, "Optimal control of nonballistic muscular movements: A constraint-based performance criterion for rising from a chair," *J. Biomech. Eng.*, vol. 117, pp. 15–26, 1995.
[10] F. Bahrami, R. Riener, and J. Quintern, "Arm-supported standing up: A comparative study," in *Proc. 2nd IFESS Conf.*, Vancouver, B.C., Canada, Aug. 1997, pp. 197–198.
[11] T. Bajd, A. Kralj, and R. Turk, "Standing-up of a healthy subject and a paraplegic patient," *J. Biomechan.*, vol. 15, pp. 1–10, 1982.
[12] S. L. Delp, "Surgery simulation: A computer graphics system to analyze and design musculoskeletal reconstructions of the lower limb," Ph.D. dissertation, Stanford Univ., Stanford, CA, 1990.
[13] A. B. Schulz, N. B. Alexander, and J. A. Ashton-Miller, "Biomechanical analysis of rising from a chair," *J. Biomechan.*, vol. 25, pp. 1383–1391, 1992.
[14] B. Markiewicz, "Analysis of the computed torque drive method and comparison with conventional position servo for a computer-controlled manipulator," Jet Prop. Lab., Pasadena, CA, Mar. 15, 1973.
[15] C. H. An, C. G. Atkeson, J. Griffiths, and J. M. Hollerbach, "Experimental evaluation of feedforward and computed torque control," *IEEE Trans. Robot. Automat.*, vol. 5, pp. 368–373, 1989.
[16] R. Kelly and R. Salgado, "PD control with computed feedforward of robot manipulators: A design procedure," *IEEE Trans. Automat.. Contr.*, vol. 10, pp. 566–571, 1994.
[17] N. de N. Donaldson and C. H. Yu, "A strategy used by paraplegics to stand up using FES," this issue, pp. 162–167.
[18] G. Khang and F. E. Zajac, "Paraplegic standing controlled by functional neuromuscular stimulation: Part I and part II," *IEEE Trans. Biomed. Eng.*, vol. 36, pp. 873–894, 1989.
[19] G. T. Yamaguchi and F. E. Zajac, "Restoring unassisted natural gait to paraplegics via functional neuromuscular stimulation: A computer simulation study," *IEEE Trans. Biomed. Eng.*, vol. 37, pp. 886–902, 1990.
[20] R. J. Jaeger, "Design and simulation of closed-loop electrical stimulation orthoses for restoration of quiet standing in paraplegia," *J. Biomechanics*, vol. 19, pp. 825–835, 1986.
[21] J. J. Abbas and H. J. Chizeck, "Feedback control of coronal plane hip angle in paraplegic subjects using functional neuromuscular stimulation," *IEEE Trans. Biomed. Eng.*, vol. 38, pp. 687–698, 1991.
[22] A. J. Mulder, P. H. Veltink, H. B. K. Boom, and G. Zilvold, "Low-level finite state control of knee joint in paraplegic standing," *J. Biomed. Eng.*, vol. 14, pp. 3–8, 1991.
[23] P. H. Veltink, personal communication.
[24] A. Isidori, *Nonlinear Control Systems*, 3rd ed. London, U.K.: Springer-Verlag, 1995.
[25] J. Quintern, R. Riener, and S. Rupprecht, "Comparison of simulation and experiments of different closed-loop strategies for FES: Experiments in paraplegics," *Art. Organs*, vol. 25, pp. 232–235, 1996.
[26] P. H. Veltink, H. J. Chizeck, P. E. Crago, and A. El-Bialy, "Nonlinear joint angle control for artificially stimulated muscle," *IEEE Trans. Biomed. Eng.*, vol. 39, pp. 368–380, 1992.
[27] H. Hatze, *Myocybernetic Control Models of Skeletal Muscle*. South Africa: University of South Africa, 1981.
[28] R. Happee, "Inverse dynamic optimization including muscular dynamics, a new simulation method applied to goal directed movements," *J. Biomechan.*, vol. 27, pp. 953–960, 1994.
[29] W. F. Dostal, "Actions of the hip muscles," *Phys. Therapy*, vol. 66, pp. 351–361, 1986.
[30] G. Nemeth and H. Ohlsen, "In vivo moment arm lengths for hip extensor muscles at different angles of hip flexion," *J. Biomechan.*, vol. 18, pp. 129–140, 1985.
[31] G. N. Duda, D. Brand, S. Freitag, W. Lierse, and E. Schneider, "Variability of femoral muscle attachments," *J. Biomechan.*, vol. 29, pp. 1185–1190, 1996.
[32] C. W. Spoor and J. L. van Leeuwen, "Knee muscle moment arms from MRI and from tendon travel," *J. Biomechan.*, vol. 25, pp. 201–206, 1992.
[33] A. E. Fick, "Ueber zweigelenkige muskeln," *Arch. Anat. Physiol. (Anat. Abt.)*, pp. 201–239, 1879.
[34] E. S. Grood, W. J. Suntay, F. R. Noyes, and D. L. Butler, "Biomechanics of the knee-extension exercise," *J. Bone Joint Surg.*, vol. 66-A, no. 5, pp. 725–733, 1984.
[35] T. M. G. J. van Eijden, E. Kouwenhoven, and W. A. Weijs, "The influence of anterior displacement of the tibial tuberiosity on patellofemoral biomechanics," *Int. Orthopaed.*, vol. 11, pp. 215–221, 1987.
[36] P. Klein, S. Mattys, and M. Rooze, "Moment arm length variations of selected muscles acting on talocrural and subtalar joints during movement: An *in vitro* study," *J. Biomechan.*, vol. 29, pp. 21–30, 1996.
[37] S. G. Rugg, R. J. Gregor, B. R. Mandelbaum, and L. Chiu, "In vivo moment arm calculations at the ankle using magnetic resonance imaging (MRI)," *J. Biomechan.*, vol. 23, pp. 495–501, 1990.
[38] C. W. Spoor, J. L. van Leeuwen, C. G. M. Meskers, A. F. Titulaer, and A. Huson, "Estimation of instantaneous moment arms of lower leg muscles," *J. Biomechan.*, vol. 23, pp. 1247–1259, 1990.

[39] M. A. Johnson, J. Polgar, D. Weightman, and D. Appleton, "Data on the distribution of fiber types in thirthy-six human muscles. An autopsy study," *J. Neurologic. Sci.*, vol. 18, pp. 111–129, 1973.
[40] J. T. Mortimer, "Motor prostheses," in *Handbook of Physiology, Nervous System II.*, V. B. Brooks, Ed., Bethesda, MD: American Physiological Society, 1981, vol. 2, pp. 155–187.
[41] H. P. Clamann, "Motor unit recruitment and the gradation of muscle force," *Phys. Therapy*, vol. 73, pp. 830–842, 1993.
[42] D. A. Winter, *Biomechanics and Motor Control of Human Movement*. New York: Wiley, 1990.
[43] J. M. Winters, "Hill-based muscle models: A system engineering perspective," in *Multiple Muscle Systems*, Winters and Woo, Eds. New York: Springer-Verlag, 1990, pp. 69–93.
[44] M. B. Reid, G. J. Grubwieser, D. S. Stokic, S. M. Koch, and A. A. Leis, "Development and reversal of fatigue in human of tibialis anterior," *Muscle Nerve*, vol. 16, pp. 1239–1245, 1993.
[45] Z. Z. Karu, W. K. Durfee, and A. M. Barzilai, "Reducing muscle fatigue in FES applications by stimulating with N-let pulse trains," *IEEE Trans. Biomed. Eng.*, vol. 42, pp. 809–817, 1995.
[46] R. Riener, J. Quintern, E. Psaier, and G. Schmidt, "Physiologically based multi-input model of muscle activation," in *Neuroprosthetics. From Basic Research to Clinical Applications*, Pedotti, Ferrarin, Quintern, and Riener, Eds. New York: Springer-Verlag, 1996, pp. 95–115.
[47] V. Zatsiorsky and V. Seluyanov, "The mass and inertia characteristics of the main segments of the human body," in *Int. Series Biomechan.*, Biomechanics VIII-B, Matsui and Kobayashi, Eds. Human Kinetics, Champaign, IL, vol. 4B, 1983, pp. 1152–1159.

Robert Riener (S'96–A'98) was born in Munich, Germany, in 1968. He received the Dipl.-Ing. degree in mechanical engineering and the Doctoral degree in engineering from the Technical University of Munich, Germany, in 1993 and 1997, respectively. His doctoral dissertation concerned modeling and control in FES.

He spent time at the University of Maryland, College Park, performing numerical simulation studies of breaking water waves as a Prof. E. Müller-Stiftung Scholar. Currently, he is a Postdoctoral Research Fellow at the Centro di Bioingegneria, Politecnico di Milano. His research interests involve the control of normal and pathological limb movements, FES, and the modeling of neuromuscular systems.

Dr. Riener is a member of ISB, IFESS, and the the Institute of Electrical and Electronics Engineers/Engineering in Medicine and Biology Society (IEEE/EMBS).

Thomas Fuhr (S'96) was born in Stuttgart, Germany, in 1968. He received the Dipl.-Ing. degree in cybernetics (Technische Kybernetik) from the University of Stuttgart in 1997. He is currently pursuing the doctoral degree at Technical University of Munich (TUM), Munich, Germany.

In 1995, he was granted an international scholarship by the Illinois Institute of Technology (I.I.T.), Chicago, IL, where he spent a year with Prof. R. J. Jaegar at the Pritzker Institute of Medical Engineering, working on functional electrical stimulation of expiratory muscles, and human ventilation control mechanisms. In 1997, he joined the Lehrstuhl für Steuerungs-und Regelungstechnik (Institute of Automatic Control) at TUM, where he developed nonlinear control strategies for closed-loop neuroprostheses of the lower extremity as a part of his Dipl.-Ing. dissertation. His areas of research include functional electrical stimulation, control, modeling and simulation of physiological systems, and nonlinear control systems.

He is a member of the Institute of Electrical and Electronics Engineers/Engineering in Medicine and Biology Society (IEEE/EMBS) and IFESS. He was awarded first prize at the I.I.T. Undergraduate Research Conference 1996.